HARVEY W. KO, JOHN S. HANSEN, and LYNN W. HART

THE APL BIOELECTROMAGNETICS LABORATORY

A laboratory has been established at APL to carry out noninvasive bioelectromagnetic measurements. Ongoing work includes localizing and characterizing epileptic sources and the development of a brain edema monitor and a bone healing monitor. The purpose of the investigations is to provide enhanced clinical diagnostic capabilities for collaborators at the Johns Hopkins Medical Institutions.

INTRODUCTION

The Bioelectromagnetics Laboratory was established at APL in 1984 as a facility dedicated to performing electromagnetic measurements of various biological systems. The technological base for investigations in the facility stems from broad theoretical, analytical, and experimental experience in electromagnetic sensors, signal processing, data acquisition and processing, and background-noise characterization.

The Bioelectromagnetics Laboratory contains a large inventory of electric and magnetic sensors, phase-lock amplifiers, spectrum analyzers, gain-phase amplifiers, and various signal-analysis and data-processing instrumentation, all linked to two PDP-11/34 computers. Approximately 450 square feet of space (Fig. 1) is used for staging various experiments and for data collection and analysis.

The principal measurements made in the laboratory are of the magnetic fields of the human body. Figure 2 is a scale of magnetic induction that places the amplitudes of human magnetic fields in context with magnetic fields that are ordinarily sensed. The magnetic field of the earth, which is the primary force in compass navigation, is on the order of 10^{-4} tesla. Urban magnetic noise, such as that produced by the motion of vehicles and stray electrical signals, is on the order of 10^{-6} tesla. Magnetic fields from the human heart, eye, and brain range between 10^{-10} and 10^{-13} tesla. Therefore, very sensitive magnetic field sensors that can sense one-billionth of the earth's steady magnetic field are required in order to analyze the magnetic fields of the human body.

A superconducting magnetometer that can achieve that degree of sensitivity is based on a device called a SQUID (superconducting quantum interference device), which is a loop of indium wire immersed in liquid helium at 4 K. At that supercooled temperature, the electrical impedance of the wire loop is practically zero. Therefore, a magnetic field sensed by the loop induces a current in the wire that has a very large value. In essence, the SQUID is an extremely sensitive ammeter.

Figure 1—A wide-angle view of APL's Bioelectromagnetics Laboratory.

The sensing loop of a superconducting magnetometer is comprised of three superconducting coils (Fig. 3). The primary coil (loop A) measures the signal under investigation and the ambient background noise. The other two coils (loops B and C) are placed far enough away from the primary signal that they can measure the ambient background noise. Under the assumption that the ambient noise sources are very far away, the magnetic field gradients from those distant sources are uniform. Therefore, the secondary magnetic sensor coils—loops B and C—can subtract the background noise from the primary signal plus the noise measured by loop A, leaving only the signal under investigation. As much as 20 to 30 decibels of background noise reduction can be achieved with this simple difference method.

THE BIOELECTROMAGNETICS MEASUREMENT

The magnetic measurement is comprised of environmental noise, biologic noise, and sensor noise in addition to the signal under investigation (Fig. 4). Environmental noise can be broken down into (a) geomagnetic noise, created by sunspot-induced magnetic fields traveling through the ionosphere, and propagating magnetic

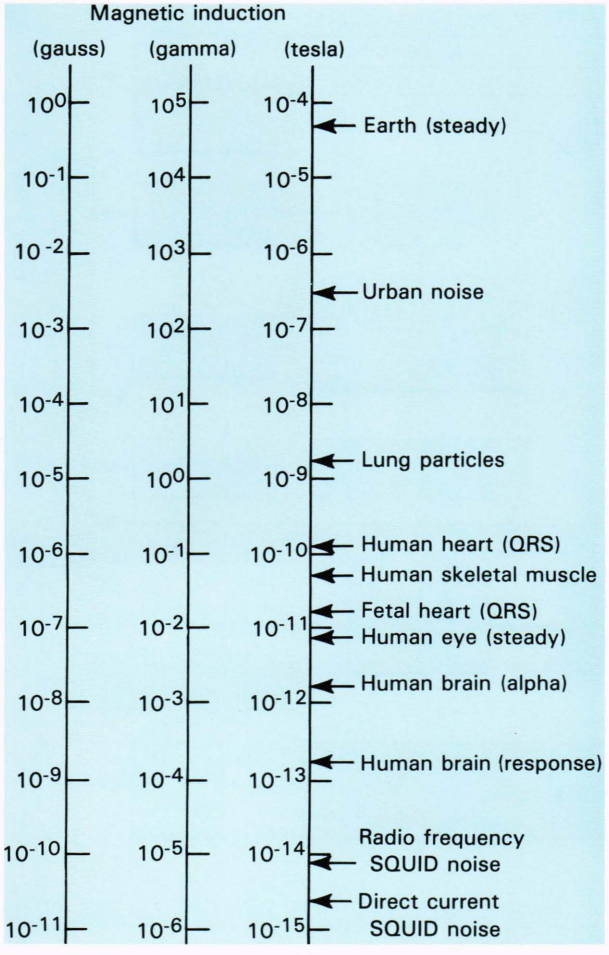

Figure 2—Magnetic fields of the human body and the earth measured in centimeter-gram-second units (gauss) and in meter-kilogram-second units (teslas).

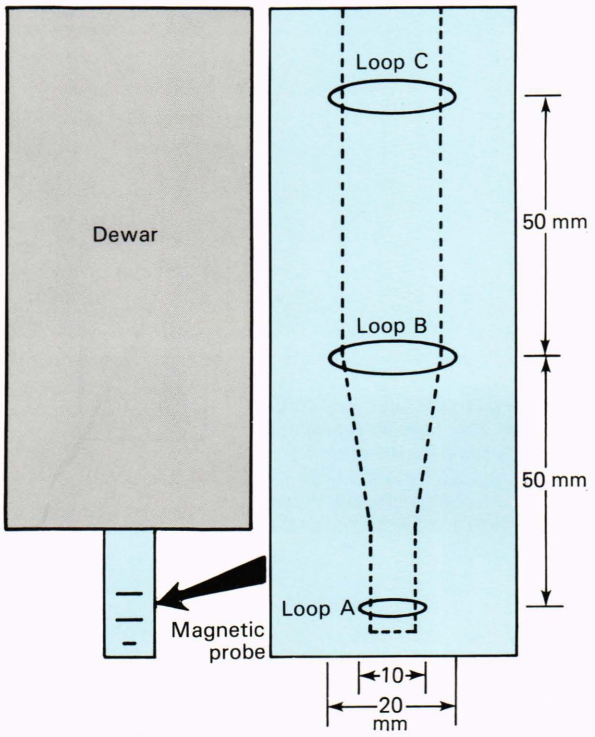

Figure 3—The SQUID coil configuration for the superconducting second differencing gradiometer used in bioelectromagnetic investigations.

Measurement = environmental noise
(geomagnetic + geologic + urban + seismic)
+ biologic noise + sensor noise + signal

Sensors	Signal processing tools
Magnetometers	Averaging
Electrodes	Fourier transforms
Motion sensors	Widrow filtering
	Wiener filtering
	Bandpass filtering
	Gram-Schmidt orthogonalization
	Notch filtering
	Nulling techniques

Figure 4—The contributors to the bioelectromagnetics measurement and the auxiliary sensors and signal processing tools required to separate the signal under investigation from various noise sources.

fields, caused by lightning strokes occurring somewhere in the earth-ionosphere waveguide; (b) geologic noise, the magnetic field that is measured when a magnetometer is moved in the presence of the stationary magnetization in geologic strata; (c) urban noise, the magnetic field arising from the motion of vehicles and stray electrical signals; and (d) seismic noise, resulting either from the vibration of metallic objects near the magnetometer or from the motion of the magnetometer itself in the presence of the stationary magnetic field of the earth. Biologic noise is defined as the magnetic field that arises from biologic responses that are not part of the primary signal (e.g., a somatosensory response). Sensor noise is the thermal noise of the sensor element itself.

In order to segregate the components of the bioelectromagnetic measurement, various auxiliary sensors are used: less sensitive magnetometers to measure urban and seismic noise, electric field electrodes to measure stray electrical noise, and motion sensors to measure the vibration of the sensor or the motion of the subject under test. Signal processing is used to combine the outputs of the primary bioelectromagnetic sensor and the auxiliary sensors to categorize the nature of the environmental noise and to differentiate it from the signal under investigation. Signal processing tools used include signal averaging, Widrow adaptive filtering, and Wiener filtering.

Figure 5 illustrates an experimental configuration that uses auxiliary sensors to remove the background noise. A human subject undergoing a test of visually evoked response or auditory evoked response is surrounded by the primary SQUID bioelectromagnetic sensor and various auxiliary sensors. On the subject's head are placed electroencephalogram (EEG) electrodes for a ground-truth measurement of the responses. The SQUID measures the magnetoencephalogram (MEG) signal. Mounted on the SQUID are fluxgate magnetometers to measure

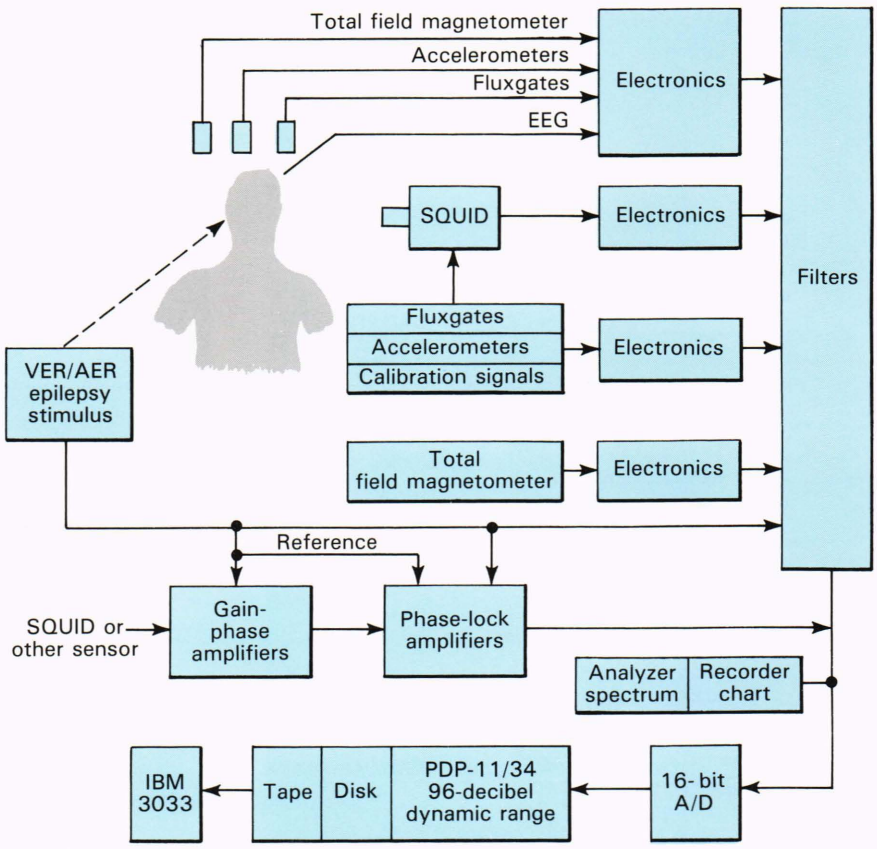

Figure 5—One particular test configuration in the bioelectromagnetic test facility used for the detection of magnetic signals from the brain during experiments on visually evoked response (VER) and auditory evoked response (AER).

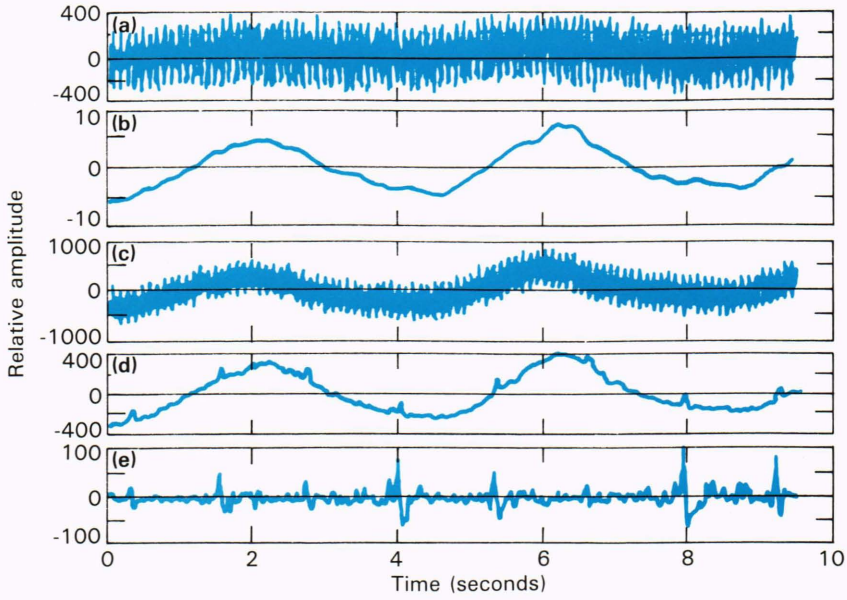

Figure 6—The use of Widrow adaptive filtering during measurements of cardiac function in the human. (a) Unfiltered accelerometer; (b) 0.5-hertz low-pass accelerometer; (c) unfiltered gradiometer; (d) 10-hertz low-pass gradiometer; and (e) gradiometer adaptively canceled by accelerometer.

ambient magnetic field changes and sensor orientation and accelerometers to measure the motion of the SQUID sensor. A total-field magnetometer to measure stray biologic signals, accelerometers to measure the motion of the subject, and fluxgate magnetometers to measure changes in the ambient magnetic field are located near the subject.

Figure 6 illustrates the benefits of noise reduction. Figure 6a shows the time series from an accelerometer placed on the stomach of a reclining subject; Fig. 6b is the same accelerometer signal after being low-pass filtered at 0.5 hertz. The SQUID magnetometer is placed over the subject's heart to measure his magnetocardiogram (MKG). Figure 6c is the output signal of the un-

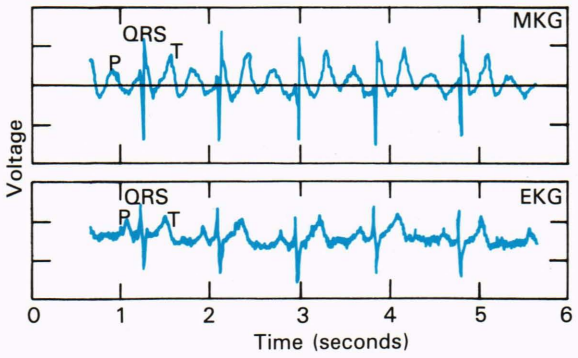

Figure 7—A comparison of an MKG and an EKG.

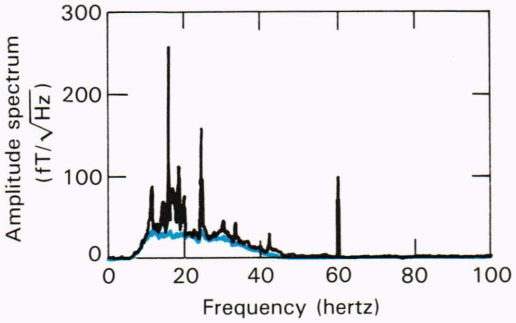

Figure 8—The magnetic field spectrum from the bioelectromagnetics gradiometer without environmental noise cancellation (black curve) and after environmental noise cancellation with six auxiliary sensors (colored curve).

filtered gradiometer, and Fig. 6d is the result of passing the unfiltered signal through a 10-hertz low-pass filter. The gradiometer registers a signal proportional to the subject's breathing, as corroborated by the accelerometer fluctuation in Fig. 6b. When the low-pass-filtered accelerometer signal is used as a reference channel in a Widrow adaptive filter and combined with the signal shown in Fig. 6d, the output of the Widrow filter shown in Fig. 6e is the MKG signal measured by the gradiometer with the breathing motion canceled.

Figure 7 compares an MKG measured by the SQUID with a standard EKG. The finestructure of the signal, identified as the P, QRS, and T components of the cardiogram, is clearly seen in both signals. The figure underscores the virtue of having a noninvasive (noncontact) method to measure cardiac function. The MKG approach might be valuable in studying the fetal heartbeat.

Figure 8 shows the ambient background magnetic field spectrum measured by the gradiometer in femtoteslas (10^{-15} tesla) per square root of the frequency in hertz. The black curve is the raw spectrum measured by the gradiometer in the frequency range from 0 to 100 hertz. Large spikes seen in the spectrum are from the SQUID's vibration in the ambient earth's field and stray electrical noise at 60 hertz. Six auxiliary sensors measure independently the sensor vibration and stray electrical noise. Their outputs are used with the Wiener filter (a coherence-type process) to obtain a corrected magnetic spectrum, as shown by the colored curve in Fig. 8. In some instances, over 40 decibels of environmental noise cancellation is obtained,[1] enabling the very small magnetic fields from the human body to be measured.

NONINVASIVE MEASUREMENT OF IN-DEPTH EPILEPTIC FOCI

Epilepsy is a condition of recurrent seizures caused by nervous system problems that affect over two million Americans. The goal of this investigation is to develop a scientifically justifiable method of noninvasively monitoring in-depth epileptic discharges in order to assess possible surgical benefits.

Figure 9 illustrates the magnetic gradiometer's ability to measure noninvasively manifestations of epilepsy in a laboratory rat. Figure 9a is the signal from the EEG voltage measured between an electrode placed deep in the right hippocampus and one placed on the left cortex. Figure 9b is the EEG voltage between an electrode

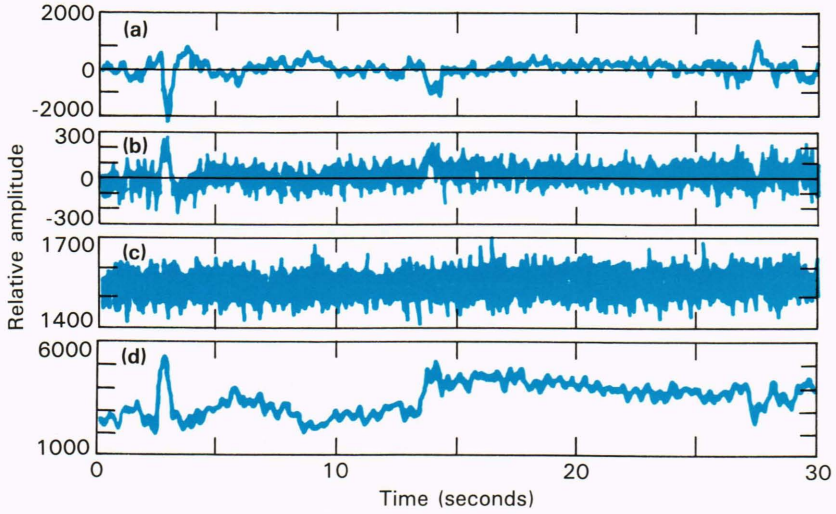

Figure 9—An MEG measured in close proximity to the rat head during the onset of epileptic seizures. (a) EEG, right hippocampus, left cortex; (b) EEG, right hippocampus, right cortex; (c) accelerometer; and (d) MEG gradiometer.

placed deep in the right hippocampus and one on the right cortex. Seizure spikes are clearly visible in both figures. Figure 9c shows the output from an accelerometer mounted on a rat holder (to ensure that rat muscle movement is not the source of any of these signals). Figure 9d shows the magnetic field from the rat brain (the MEG) as measured by the gradiometer, which is in close proximity to the rat head. The MEG magnetic activity can be clearly seen at the time of occurrence of the EEG epileptic spikes.

The specific objectives of the investigation are to determine the degree of localization attainable using state-of-the-art magnetometers in an ideal in-vitro experiment and to measure in-depth epileptic sources in vivo, particularly those not seen by the surface EEG. The investigation is done in three phases. In the first, the degree of localization in vitro is determined by means of the SQUID MEG sensor (i.e., the gradiometer) for known geometric cavities mimicking the head, with solutions of known conductivity and with calibrated sources of known size and location. The shape of the geometric cavity, the signal-to-noise ratio, and the number of measurement stations in the experiment are varied to determine the localization error as a function of those parameters.

The second phase involves introducing a calibrated electric source inside a living animal brain to determine the degree of MEG localization obtained for the known source at a known location within the real asymmetrical brain with its inhomogeneous conductivity. The third phase involves the study of natural epileptiform discharges in the living animal brain.

Figure 10 shows the in-vitro apparatus placed underneath the superconducting gradiometer sensor. The electric dipole can be seen at the center of the glass sphere, which is filled with a conducting saline solution. A laser is used to align both the dipole and the sphere relative to the position of the gradiometer.

In Fig. 11, predictions of the theoretical magnetic field gradients for the gradiometer signal are plotted as a function of gradiometer location measured in degrees from the vertical. Each curve (normalized in amplitude) is a plot of the magnetic field variation as a function of the angular position of the gradiometer for different spacings between the center of the sphere and the dipole. The gradient magnetometer is located 10 centimeters from the sphere's center. The figure shows that the location of the peak of the magnetic field in degrees from the vertical can be used to deduce the position of the dipole.

Results of this in-vitro measurement with the spherical container are given in Fig. 12. Here, an analysis algorithm used with the data has deduced the dipole to be located at 0.0109 meter; the true dipole location is 0.0100 meter. This illustrates that the dipole can be located to an accuracy of within 1 millimeter. The experiments have shown that at least a 10-decibel signal-to-noise ratio is required to obtain this degree of localization. More than eight data points are required with a 10-decibel signal-to-noise ratio, but only about four data points are needed if the signal-to-noise ratio is raised to 40 decibels.[2]

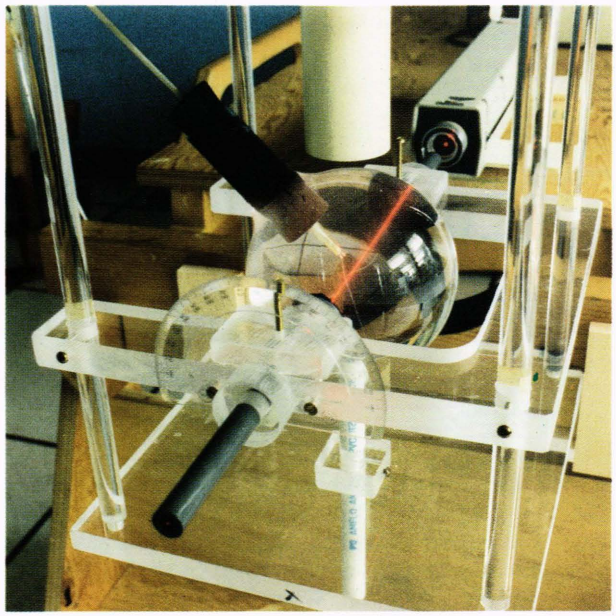

Figure 10—The spherical in vitro apparatus used to quantify the degree of localization of a dipole source located at the center of the sphere.

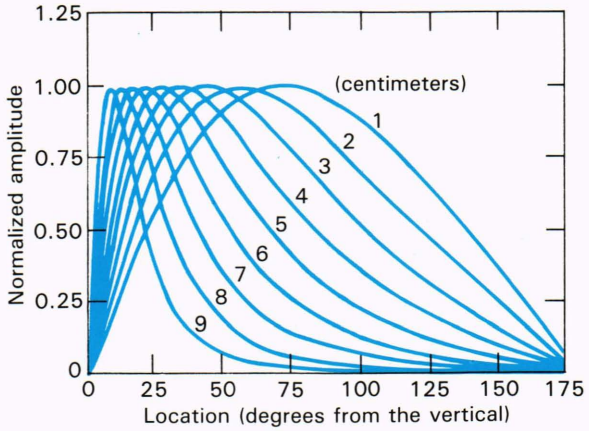

Figure 11—Theoretical gradient magnetic field predictions given as the normalized amplitude of magnetic field as a function of the angular rotation from the vertical. The magnetometer is located 10 centimeters from the sphere center. The curves are parameterized to the location of the dipole from the sphere's center.

NONINVASIVE MONITORING OF BRAIN EDEMA

Brain edema is the life-threatening increase of brain volume due to an increase in water, protein, and sodium content. It can be caused by a variety of circumstances, ranging from physical injury to drug abuse. The clinical problem presented to APL investigators is that at present there is no easy way to continuously monitor brain edema. State-of-the-art continuous monitoring techniques rely on a measurement of intracranial pressure. Furthermore, computer tomography, nuclear magnetic resonance, and position emission tomography scans

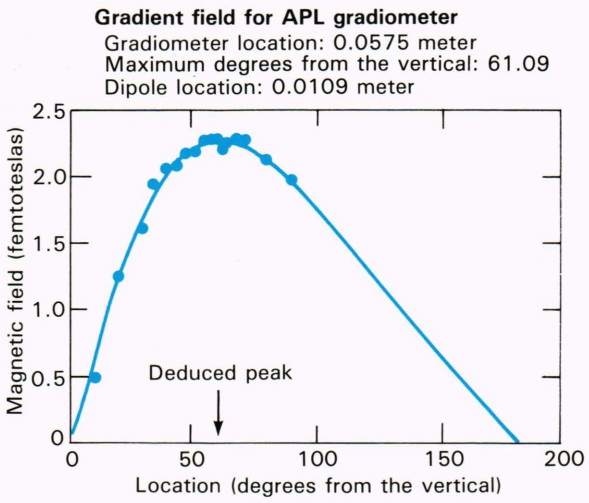

Figure 12—Experimental results for the localization of an electric dipole located 1 centimeter from the center of the in vitro sphere apparatus.

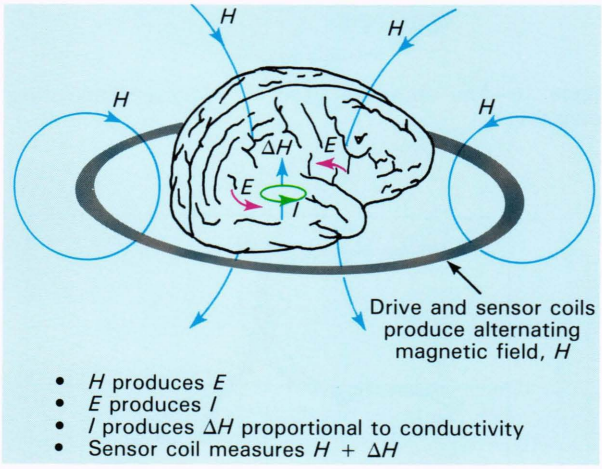

Figure 13—The physical principles of the noninvasive measurement of brain impedance, showing the detection of secondary magnetic fields produced by induced eddy currents within the brain.

are not suitable for frequent repetition. The goal of the investigation is to develop a safe, noninvasive procedure to monitor the onset and progression of brain edema at the bedside.

Figure 13 illustrates the basic idea behind the noninvasive measurement of brain edema. The technique relies on the assumption that the electrical conductivity of edematous fluid is different from that of normal brain tissue; therefore, the plan is to monitor electrical impedance changes within the brain. A coil is placed about the brain, producing an alternating magnetic field, H, which, in turn, produces an alternating electric field, E. The electric field produces small eddy currents, I, that flow through the brain. They, in turn, reradiate a smaller magnetic field, ΔH, that is proportional to the conductivity of the brain medium. The sensor coil measures the primary magnetic field, H, plus the eddy-current-produced magnetic field, ΔH.

Table 1—Approximate conductivities.

Matter	*Conductivity (siemens/meter)*
Seawater	5.0
Cerebrospinal fluid	1.5
Blood	0.6
Muscle	0.5
Skin	0.4
Brain gray matter	0.2
Brain white matter	0.1
Bone	0.05

(a)

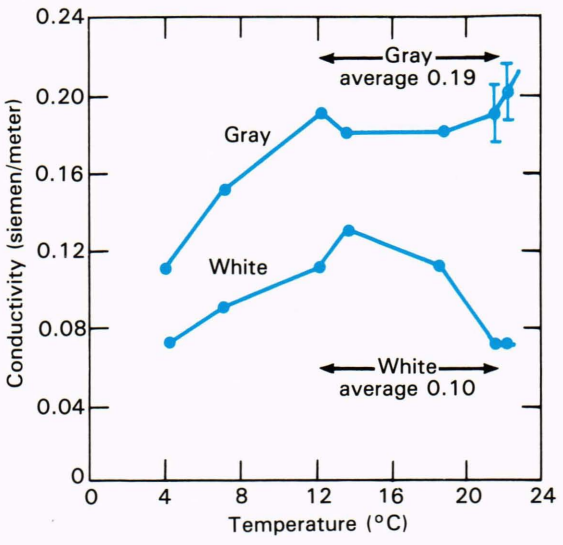

(b)

		Temperature (°C)		
		12	18	20
White	Normal	0.15 ±0.03	0.15 ±0.01	0.14 ±0.02
	Edematous	0.16 ±0.01	0.18 ±0.01	0.18 ±0.01
Gray	Normal	0.20 ±0.02	0.21 ±0.02	0.22 ±0.02
	Edematous	0.38 ±0.04	0.30 ±0.07	0.36 ±0.07

Figure 14—Experimental results for the electrical impedance of (a) white and gray normal rabbit brain at 2 megahertz and (b) white and gray normal and edematous rabbit brain at 2 and 4 megahertz.

Table 1 lists electrical conductivities measured in biological systems by various investigators. Biological conductivities range from less than 0.05 to approximately 1.5 siemens per meter. Other investigators have cataloged normal brain white matter as having a conductivity on the order of 0.1 siemen per meter and normal brain gray matter approximately 0.2 siemen per meter. The hypo-

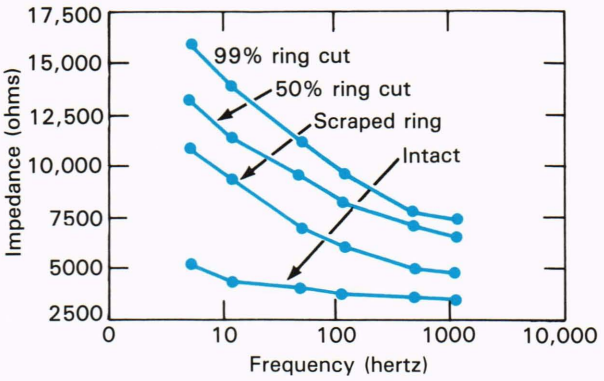

Figure 15—Experimental results for the electrical impedance of the human tibia as a function of frequency and parameterized to the extent of a ring cut around the bone.

thesis that edematous fluid would have a greater conductivity than normal gray and normal white brain matter has been substantiated by our measurements.

In collaboration with the Departments of Neurosurgery and Oncology at the Johns Hopkins Medical Institutions, APL measured the conductivities of both normal and edematous rabbit brain tissues. The results are given in Fig. 14. Figure 14a indicates the variations in the conductivity at 2 megahertz of normal white and normal gray matter of rabbit brain as a function of temperature. Figure 14b presents the results of the conductivity measurement of white and gray matter of a rabbit brain with regions of normal and edematous tissue. The brain edema is a result of a radioisotope-induced brain tumor. Results are given for three different temperatures, and the conductivity values are for frequencies of 2 and 4 megahertz. They indicate that the edematous tissue has a conductivity ranging between the values for normal brain tissue and for cerebrospinal fluid.[3] Therefore, it is hoped that further investigations of this noninvasive measure of brain conductivity will lead to successful monitoring of brain edema.

QUANTIFICATION OF BONE HEALING

The goal of the investigation is to monitor and gauge noninvasively the mechanical integrity of a healing bone fracture. At present, no such method exists.

Figure 15 gives results from the measurement of the electrical impedance of a human cadaver bone. Electrodes are placed on the cadaver bone to measure impedance changes in the bone as a function of frequency, parameterized to the extent of the induced fracture caused by sawing around the circumference of the bone. At any given frequency, the impedance increases as the extent of the fracture increases (or, equivalently, the electrical conductivity of the bone decreases as the extent of the fracture increases). The changes in electrical impedance or electrical conductivity in these experiments suggest that the same method of measuring biological impedance previously described for brain edema might be applied to measure the extent of bone healing.

A measurement of a simulated bone is illustrated in Fig. 16; a nonconducting plastic rod with a variable gap

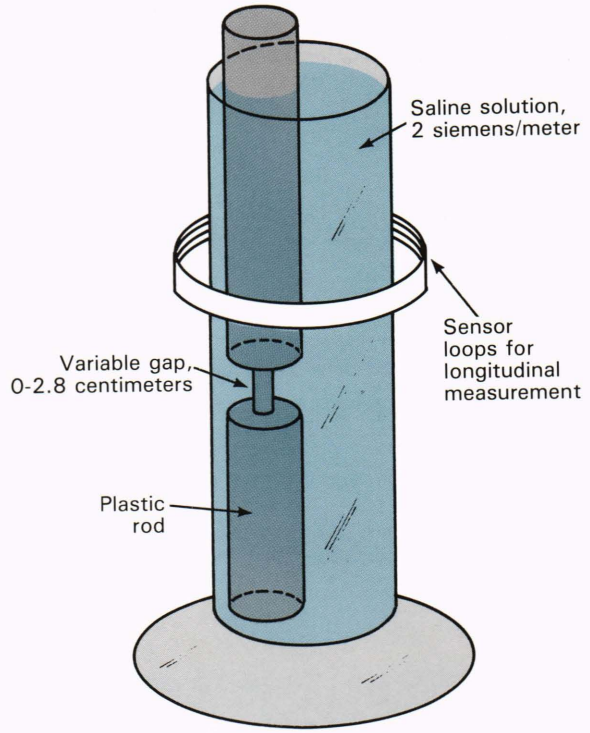

Figure 16—The apparatus used for simulated-bone measurements.

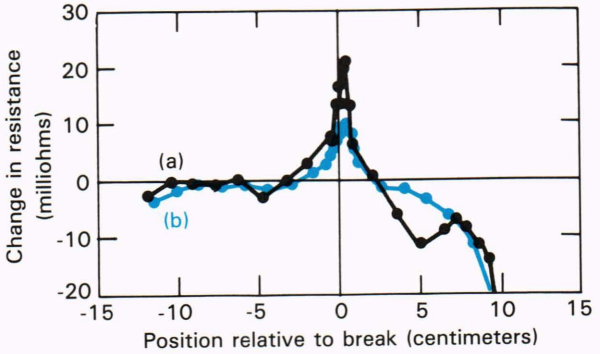

Figure 17—Experimental results from the measurement of changes in sensor coil impedance during the measurement of the simulated bone for a break size of 0.7 centimeter (black curve) and for a break size of 0.3 centimeter (colored curve).

is placed inside a tall beaker filled with saline solution. The variable gap simulates the bone fracture site. A coil wrapped around the apparatus provides a way to measure the change in resistance in the sensor loop system, which is proportional to the change in conductivity measured at the fracture site. Figure 17 gives the resistance change in milliohms as a function of position relative to the break for a break size of 0.7 centimeter (the black curve) and 0.3 centimeter (the colored curve).

SUMMARY

The APL Bioelectromagnetics Laboratory is a resource for several biomedical investigations. Of equal

value is the wealth of experience offered by the investigators in the areas of medical science and electromagnetics technology. The theories, experimental procedures, signal and data processing techniques, and sensor technology are unclassified by-products of other Department of Defense funded efforts at APL. The three investigations discussed are funded as a result of past APL Independent Research and Development initiatives performed in collaboration with investigators from the University of Colorado, the University of California at Los Angeles, and the Johns Hopkins Medical Institutions.

REFERENCES

[1] J. S. Hansen, D. A. Bowser, and H. W. Ko, "Adaptive Noise Cancellation in Neuromagnetic Measurement Systems," *Il Nuovo Cimento* **2D**, 203-213 (1983).

[2] J. S. Hansen, H. W. Ko, R. S. Fisher, and B. Litt, "Practical Limits on the Biomagnetic Inverse Process Determined from in-Vitro Measurements in Spherical Conducting Volumes," Biomagnetic Inverse Problem Study Conf., Milton Keynes, England (Apr 1986).

[3] D. M. Long and H. W. Ko, "Quantification of Brain Edema by Measurement of Brain Conductivity," 6th International Symp. on Brain Edema, Tokyo (Nov 7-10, 1984); also in *Brain Edema*, Y. Inaba, ed., pp. 632-637 (1985).

ACKNOWLEDGMENTS—The authors would like to acknowledge the collaboration of our colleagues at the Johns Hopkins Medical Institutions: R. S. Fisher, Director, Adult Seizure Clinic; D. M. Long, Chief of Neurosurgery; and A. F. Brooker, Chief of Adult Orthopedic Surgery. Measurements and analyses at APL would not have succeeded without the help of J. P. Skura, B. Litt, and J. H. Meyer, Jr. Special thanks go to J. R. Austin, R. W. Flower, M. H. Friedman, R. A. Meyer, and R. Johns for their support and encouragement.

THE AUTHORS

HARVEY W. KO (left) was born in Philadelphia in 1944 and received the B.S.E.E. (1967) and Ph.D. (1973) degrees from Drexel University. During 1964-65, he designed communications trunk lines for the Bell Telephone Co. In 1966, he performed animal experiments and spectral analysis of pulsatile blood flow at the University of Pennsylvania's Presbyterian Medical Center. After joining APL in 1973, Dr. Ko investigated analytical and experimental aspects of ocean electromagnetics, including ELF wave propagation and magnetohydrodynamics. Since 1981, he has been examining radar wave propagation in coastal environments and bioelectromagnetics. He is now on the Technical Staff of the Submarine Technology Division.

JOHN S. HANSEN (right) is a member of the Space Analysis and Computation Group in APL's Space Department. He received B.A. degrees in mathematics and physics from the University of Utah in 1971 and a Ph.D. in experimental physics from the University of Durham, England, in 1975. He is currently completing an M.S. in computer science at The Johns Hopkins University. At Durham, Dr. Hansen investigated cosmic ray effects, and, while teaching at the University of Nottingham, he investigated extremely high energy cosmic ray activity (1974-76). In 1977, he operated a neutrino experimental station under Lake Erie.

In 1978, Dr. Hansen joined the Magnetics Group in APL's Submarine Technology Department, where he has specialized in systems engineering, software engineering, and signal processing. He has designed, specified, and operated several experimental systems, including the development of a five-axis superconducting magnetic gradiometer system (1983-85) and APL's Bioelectromagnetics Laboratory (1985). Since 1983, he has been interested in the application of electromagnetic technology and signal processing technology to biomedical noninvasive measuring and monitoring. Currently, he is the U2 spectrograph systems engineer at the Bioelectromagnetics and Signal Processing Laboratory established at APL in 1985.

LYNN W. HART (center) is a member of APL's Principal Professional Staff. Born in Logan, Utah, in 1942, he received the B.S. degree in physics from Brigham Young University in 1967 and the Ph.D. degree in physics from Iowa State University in 1971. He worked as a postdoctoral fellow at Kent State University from 1971-72 and at APL from 1972-73. In 1973, he joined APL's senior technical staff in the Space Department. Dr. Hart later became a member of the Submarine Technology Division, where he conducted electromagnetics research sponsored by the Navy in the SSBN Security Technology Program. He continues electromagnetics research for Navy sponsors and also pursues biomedical investigations. His other areas of research have included magnetic properties of rare-earth elements, transport properties of air pollutants through porous media, and determinations of chemical rate constants in flames. Dr. Hart is a member of Phi Kappa Phi, Sigma Xi, and the American Physical Society.